Article

Molecular Tectonics: Control of Reversible Water Release in Porous Charge-Assisted H-Bonded Networks

Pierre Dechambenoit, Sylvie Ferlay, Nathalie Kyritsakas, and Mir Wais Hosseini

J. Am. Chem. Soc., **2008**, 130 (50), 17106-17113 • DOI: 10.1021/ja806916t • Publication Date (Web): 14 November 2008

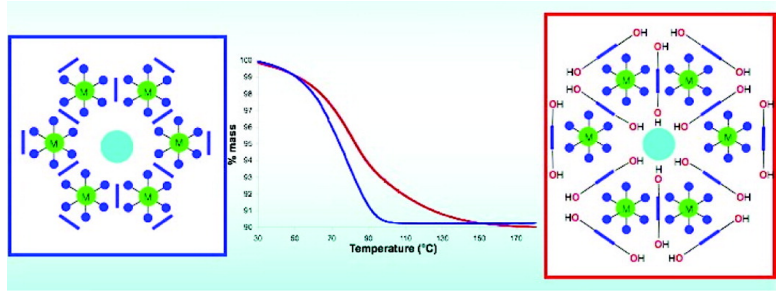

J|A|C|S
ARTICLES

Published on Web 11/14/2008

Molecular Tectonics: Control of Reversible Water Release in Porous Charge-Assisted H-Bonded Networks

Pierre Dechambenoit, Sylvie Ferlay,* Nathalie Kyritsakas, and Mir Wais Hosseini*

Laboratoire de Chimie de Coordination Organique, UMR CNRS 7140, Université Louis Pasteur, Institut Le Bel, 4 rue Blaise Pascal, F-67000 Strasbourg, France

Received September 1, 2008; E-mail: hosseini@chimie.u-strasbg.fr; ferlay@chimie.u-strasbg.fr

Abstract: The combinations of bisamidium dicationic tectons **1**-2H$^+$ and **2**-2H$^+$ bearing two OH groups as additional H-bond donor/acceptor sites with $[M(CN)_6]^{3-}{}_2$ (M = Fe, Co, Cr) anions lead to the formation of robust porous crystals (decomposition temperature in the range of 240−300 °C) offering channels occupied by water molecules. The release and uptake of solvent molecules takes place through a reversible single crystal-to-single crystal transformation. Importantly, the temperature of dehydration can be increased by *ca* 40 °C through the decoration of the channels by introduction of OH groups on the backbone of the organic tecton.

1. Introduction

Molecular organization through self-assembly processes,[1] that is, spontaneous generation of complex molecular architectures from molecular units through reversible intermolecular interactions is continuously attracting interest. In the solid state, molecular crystals are defined as periodic 3-D assemblies of molecules. By considering crystals as supramolecular[2] assemblies,[3] that is, looking at molecular components of crystals as construction units or tectons,[4,5] one may, by design, control some of the intertectons interactions through molecular recognition events. Owing to the periodic nature of crystals, the recognition patterns must be regarded as structural nodes[6] and depending on the number (1, 2, 3) of translations operating on them, this type of molecular crystals may be regarded and analyzed as **X**-D (**X** = **1**, **2**, **3**) molecular networks.[7] Concerning the recognition patterns in the case of purely organic tectons,[6] many different types such as inclusion processes mainly based on van der Waals interaction,[8] H-bonding[9] and coordination bonding[10] have been explored over the last two decades. Although at the initial steps of this approach, investigators were interested in the understanding and control of structural features of molecular networks in the crystalline phase, *i.e.* mainly the connectivity patterns, since a decade, considerable effort has been invested in obtaining molecular crystals with specific properties in the area of optics,[11] magnetism[12] or porosity.[13] In terms of applications, the control of porosity is an important issue since it may be applied to storage, separation and catalysis. The main challenges here are (i) to develop design principles allowing to generate thermally robust porous materials capable of exchanging the guest molecules without loss of structural integrity and crystallinity, (ii) to control, through the nature of the backbone, the properties of the porous architecture, in particular pore size, shape and polarity. Although H-bonds have been often used in the area of crystal engineering,[9] with the exception of few examples,[14] the majority of reported porous

(1) (a) Whitesides, G. M.; Mathias, J. P.; Seto, T. *Science* **1991**, *254*, 1312–1319. (b) Lindsey, J. S. *New J. Chem.* **1991**, *15*, 153–180.
(2) Lehn, J.-M. *Supramolecular Chemistry, Concepts and Perspectives*; VCH: Weinheim, 1995.
(3) (a) Schmidt, G. M. *J. Pure Appl. Chem.* **1971**, *27*, 647–678. (b) Dunitz, J. D. *Pure Appl. Chem.* **1991**, *63*, 177–185. (c) Dunitz, J. D. *Perspectives in Supramolecular Chemistry*; Desiraju, G. R., Ed.; Wiley: New York, 1996; Vol. 2. (d) Desiraju, G. D. *Crystal Engineering: The Design of Organic Solids*; Elsevier: New York, 1989.
(4) (a) Simard, M.; Su, D.; Wuest, J. D. *J. Am. Chem. Soc.* **1991**, *113*, 4696–4698. (b) Mann, S. *Nature* **1993**, *365*, 499–505. (c) Wuest, J. D. *Chem. Commun.* **2005**, 5830–5837.
(5) (a) Hosseini, M. W. *CrystEngComm* **2004**, *6*, 318–322. (b) Hosseini, M. W. *Acc. Chem. Res.* **2005**, *38*, 313–323. (c) Hosseini, M. W. *Chem. Comm.* **2005**, 582–583.
(6) Desiraju, G. R. *Angew. Chem., Int. Ed.* **1995**, *34*, 2311–2327.
(7) (a) Etter, M. C. *Acc. Chem. Res.* **1990**, *23*, 120126;(b) Fowler, F. W.; Lauher, J. W *J. Am. Chem. Soc.* **1993**, *115*, 5991–6000.
(8) Hosseini, M. W.; De Cian, A. *Chem. Commun.* **1998**, 727–733.
(9) (a) Jeffrey, G. A. *An Introduction to Hydrogen Bonding*; Oxford University Press: Oxford, 1997. (b) Taylor, R.; Kennard, O. *Acc. Chem. Res.* **1984**, *17*, 320–326. (c) Ermer, O. *J. Am. Chem. Soc.* **1988**, *110*, 3747–3754. (d) Aakeröy, C. B.; Seddon, K. R. *Chem. Soc. Rev.* **1993**, *22*, 397–407. (e) Subramanian, S.; Zaworotko, M. J. *Coord. Chem. Rev.* **1994**, *137*, 357–401. (f) Lawrence, D. S.; Jiang, T.; Levett, M. *Chem. Rev.* **1995**, *95*, 2229–2260. (g) Stoddart, J. F.; Philip, D. *Angew. Chem., Int. Ed. Engl.* **1996**, *35*, 1154–1196. (h) Fredericks, J. R.; Hamilton, A. D. In *Comprehensive Supramolecular Chemistry*; Atwood, J. L., Davis, J. E., Macnico, D. D., Vögtle, F., Eds.; Elsevier: Oxford, 1996; Vol. 9, pp 565−594. (i) Braga, D.; Grepioni, F. *Acc. Chem. Res.* **2000**, *33*, 601–608.
(10) (a) Batten, S. R.; Robson, R. *Angew. Chem., Int. Ed.* **1998**, *37*, 1460–1494. (b) Blake, A. J.; Champness, N. R.; Hubberstey, P.; Li, W.-S.; Withersby, M. A.; Schröder, M. *Coord. Chem. Rev.* **1999**, *193*, 117–138. (c) Hosseini, M. W. In *NATO ASI Series*; Braga, D. Grepiono, F., Orpen, G., Serie, C., Eds.;Kluwer: Dordrecht, Netherlands, 1999; Vol. 538, pp 181−208. (d) Moulton, B.; Zaworotko, M. J. *Chem. Rev.* **2001**, *101*, 1629–1658. (e) Eddaoui, M.; Moler, D. B.; Li, H.; Chen, B.; Reineke, T. M.; O'Keeffe, M.; Yaghi, O. M. *Acc. Chem. Res.* **2001**, *34*, 319–330. (f) Swiergers, G. F.; Malefetse, T. J. *Chem. Rev.* **2000**, *100*, 3483–3538. (g) Janiak, C. *Dalton Trans.* **2003**, 2781–2804. (h) Kitagawa, S. *Angew. Chem. Int Ed.* **2004**, *43*, 2334–2375. (i) Ferey, G. *Chem. Soc. Rev.* **2008**, *37*, 191–214.
(11) (a) Sliwa, M.; Letard, S.; Malfant, I.; Nierlich, M.; Lacroix, P. G.; Asahi, T.; Masuhara, H.; Yu, P.; Nakatani, K. *Chem. Mater.* **2005**, *17*, 4727–4735. (b) Datta, A.; Pati, S. K. *Chem. Soc. Rev.* **2006**, *35*, 1305–1323. (c) Cariati, E.; Macchi, R.; Robert, D.; Ugo, R.; Galli, S.; Casati, N.; Macchi, P.; Sironi, A.; Bogani, L.; Caneschi, A.; Gatteschi, D. *J. Am. Chem. Soc.* **2007**, *129*, 9410–9420.

10.1021/ja806916t CCC: $40.75

crystalline materials are based on coordination networks or metallo-organic frameworks (MOFs).[15]

For the generation of porous crystals based on molecular networks, H-bonding, owing to its rather directional nature,[7a,9a,b] is an interesting tool for the design of the structural nodes. However, this type of interactions is rather weak. To form robust architectures, one may combine H-bonding with less directional electrostatic charge−charge interactions. This type of recognition pattern is called charge-assisted H-bonds and was deeply investigated by the Ward's group using a combination of guanidinium as the cationic tecton and sulfonate derivatives as anionic partners.[16] Furthermore, the same group has elegantly demonstrated the possibility of modulating the pore size through the nature and length of the pillars.[16h]

We have also investigated charge-assisted H-bonding by combining amidinium derivatives and a variety of anionic tectons.[5b,17−21]

The design of porous crystals requires several levels of analysis and organization: (i) tectons (shape, size, number and localization of interaction sites, number and nature of auxiliary sites decorating the empty space), (ii) network formed by mutual interconnection of tectons (dimensionality (1−3D), polarity and porosity), (iii) crystal obtained by the packing of networks (porosity, interpenetration, noninterpenetration), and (iv) pores (size, shape, accessibility, polarity, hydrophilicity, hydrophobicity).

For porous crystals, one of the most challenging tasks remains the control of interactions between channels and guest molecules. In other terms, the design of proper tectons bearing within their backbones both recognition sites taking part in the formation of the network and furthermore auxiliary groups pointing toward the interior of channels and thus allowing to decorate the empty space.

In this contribution, we report an unprecedented study demonstrating the fine control of reversible water release and uptake by designed robust porous crystals based on the combination of the cationic tecton **2**-2H$^+$ bearing two OH groups as auxiliary sites and hexacyanometallate anions (Figure 1).

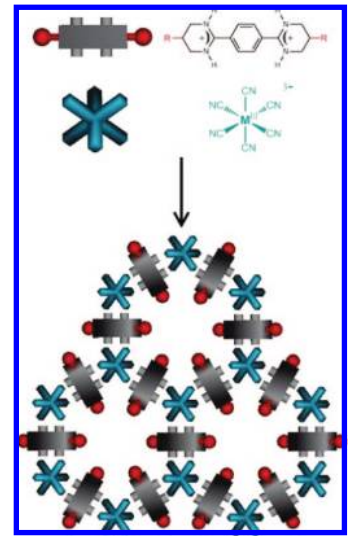

Figure 1. Schematic representation of neutral 2-D honeycomb type charge-assisted H-bonded networks presenting hexagonal cavities formed upon combining dicationic tectons such as **X**-2H$^+$, (**X** = **1**−**3**) with $[M^{III}(CN)_6]^{3-}$ (M = Fe, Co, Cr) complex anions.

2. Experimental Section

2.1. Materials. The chemicals purchased from commercial sources were used without further purification.

Synthesis of 1−2HCl. The initial synthesis of **1**-2HCl was based on the Oxley and Short method consisting in the condensation in the solid state of the monotosylate salt of 1,3-diaminopropane with 1,4-dicyanobenzene affording the dicationic compound **1** as its tosylate salt.[22] However, we found a more efficient alternative preparation based on the use of P_2S_5 as catalyst.[23]

1,4-Dicyanobenzene (1.73 g, 13.6 mmol), 2.00 g (27.2 mmol, 2 equiv) of 1,3-diaminopropane, and *ca* 20 mg of P_2S_5 were heated at 120 °C and stirred under a gentle flux of argon during 2 h. The resulting solid was cooled to 50 °C, grounded at r.t., and then acidified with an aqueous solution of HCl (1N) until pH ∼1 was reached. After stirring during 15 min, the mixture was filtered. The filtrate was evaporated leaving a slightly yellowish solid. The latter was dissolved in distilled water. Upon air evaporation, large yellowish crystals of pure compound **1**-2HCl were obtained (70%

(12) (a) Miller, J. S. *Inorg. Chem.* **2000**, *39*, 4392–4408. (b) Andruh, M. *Chem. Commun.* **2007**, 2565–2567. (c) Maspoch, D.; Ruiz-Molina, D.; Veciana, J. *Chem. Soc. Rev.* **2007**, *36*, 770–818.

(13) (a) Ockwig, N. W.; Delgado-Friedrichs, O.; O'Keefe, M.; Yaghi, O. M. *Acc. Chem. Res.* **2005**, *38*, 176–182. (b) Rosseinsky, M. J. *Microporous Mesoporous Mater.* **2004**, *73*, 15–30. (c) Kitagawa, S.; Kitaura, R.; Noro, S. *Angew. Chem., Int. Ed.* **2004**, *43*, 2334–2375. (d) Férey, G. *Acc. Chem. Res.* **2005**, *38*, 217–225.

(14) (a) Brunet, P.; Simard, M.; Wuest, J. D. *J. Am. Chem. Soc.* **1997**, *119*, 2737–2738. (b) Demers, E.; Maris, T.; Wuest, J. D. *Cryst. Growth Des.* **2005**, *5*, 1227–1235. (c) Trolliet, C.; Poulet, G.; Tuel, A.; Wuest, J. D.; Sautet, P. *J. Am. Chem. Soc.* **2007**, *129*, 3621–3626. (d) Yaghi, O. M.; Li, H.; Groy, T. L. *J. Am. Chem. Soc.* **1996**, *118*, 9096–9101. (e) Aakeröy, C. B.; Beatty, A. M.; Leinen, D. S. *Angew. Chem., Int. Ed.* **1999**, *38*, 1815–1819. (f) Maspoch, D.; Domingo, N.; Ruiz-Molina, D.; Wurst, K.; Tejada, J.; Rovira, C.; Veciana, J. *J. Am. Chem. Soc.* **2004**, *126*, 730–731. (g) Uemura, K.; Kitagawa, S.; Fukui, K.; Saito, K. *J. Am. Chem. Soc.* **2004**, *126*, 3817–3828. (h) Stephenson, M. D.; Hardie, M. G. *CrystEngComm* **2007**, *9*, 496–502.

(15) (a) Bradshaw, D.; Claridge, J. B.; Cussen, E. J.; Prior, T. J.; Rosseinsky, M. J. *Acc. Chem. Res.* **2005**, *38*, 273–282. (b) Kitagawa, S.; Uemura, K. *Chem. Soc. Rev.* **2005**, *34*, 109–119. (c) Navarro, J. A. R.; Barea, E.; Galindo, M. A.; Salas, J. M.; Romero, M. A.; Quiros, M.; Masciocchi, N.; Galli, S.; Sironi, A.; Lippert, B. *J. Solid State Chem.* **2005**, *178*, 2436–2451. (d) Shimizu, G. K. H. *J. Solid State Chem.* **2005**, *178*, 2519–2526.

(16) (a) Russell, A.; Etter, M. C.; Ward, M. D. *J. Am. Chem. Soc.* **1994**, *116*, 1941–1952. (b) Russell, V. A.; Evans, C. C.; Li, W.; Ward, M. D. *Science* **1997**, *276*, 575–579. (c) Russell, V. A.; Ward, M. D. *J. Mater. Chem.* **1997**, *7*, 1123–1133. (d) Kepert, C. J.; Hesek, D.; Beer, P. D.; Rosseinsky, M. J. *Angew. Chem., Int. Ed.* **1998**, *37*, 3158–3160. (e) Holman, K. T.; Martin, S. M.; Parker, D. P.; Ward, M. D. *J. Am. Chem. Soc.* **2001**, *123*, 4421–4424. (f) Holman, K. T.; Pivovar, A. M.; Ward, M. D. *Science* **2001**, *294*, 1907–1911. (g) Dalrymple, S. A.; Shimizu, G. K. H. *J. Am. Chem. Soc.* **2007**, *129*, 12114–12116. (h) Horner, M. J.; Holman, K. T.; Ward, M. D. *J. Am. Chem. Soc.* **2007**, *129*, 14640–14660.

(17) Hosseini, M. W. *Coord. Chem. Rev.* **2003**, *240*, 157–166.

(18) Paraschiv, C.; Ferlay, S.; Hosseini, M. W.; Bulach, V.; Planeix, J.-M. *Chem. Comm* **2004**, 2270–2271.

(19) (a) Ferlay, S.; Bulach, V.; Félix, O.; Hosseini, M. W.; Planeix, J.-M.; Kyritsakas, N. *CrystEngComm* **2002**, 447–453. (b) Dechambenoit, P.; Ferlay, S.; Hosseini, M. W.; Kyritsakas, N. *Chem. Commun.* **2007**, 4626–4627.

(20) Ferlay, S.; Holakovsky, R.; Hosseini, M. W.; Planeix, J.-M.; Kyritsakas, N. *Chem. Comm* **2003**, 1224–1225.

(21) (a) Ferlay, S.; Félix, O.; Hosseini, M. W.; Planeix, J.-M.; Kyritsakas, N. *Chem. Comm.* **2002**, 702–703. (b) Dechambenoit, P.; Ferlay, S.; Hosseini, M. W.; Planeix, J.-M.; Kyritsakas, N. *New J. Chem.* **2006**, *30*, 1403–1410.

(22) Félix, O.; Hosseini, M. W.; De Cian, A.; Fischer, J. *New J. Chem.* **1997**, *21*, 285–288.

(23) Lever, A. B. P.; Ramaswamy, B. S.; Simonsen, S. H.; Thompson, L. K. *Can. J. Chem.* **1970**, *48*, 3076–3088.

yield). ^{1}H NMR (D_2O + *t*BuOH, 300 MHz, 25 °C, ppm): 2.13 (q, 4H, J = 5.8 Hz, $CH_2(CH_2-N)_2$); 3.62 (t, 8H, J = 5.8 Hz CH_2-N); 7.88 (s, 4H, *CH* arom.); ^{13}C NMR (D_2O + *t*BuOH, 75 MHz, 25 °C, ppm): 18.1 ($CH_2-CH_2-CH_2$); 39.7 (CH_2-NH_2); 128.9 (*CH* arom.); 133.6 (*C* arom.); 160.2 (N−*C*−N). The solid state structure of **1**-2HCl have been previously determined.[22]

Synthesis of 2−2HCl. For the compound **2**-2HCl, both the synthesis and crystal structure have been previously reported.[19b]

Synthesis of (1−2H$^+$)$_3$(M[(CN)$_6$]$^{3-}$)$_2$·7H$_2$O) (M = Cr, Fe or Co). To an aqueous solution (distilled, 100 mL) of $K_3M(CN)_6$ (100 mg, 0.30 mmol) an aqueous solution (distilled, 100 mL) of **1**-2HCl. $4H_2O$ (180 mg, 0.465 mmol) was added. After two days, crystalline material was obtained. The latter was filtered and dried in air affording the desired solid material in *ca* 60% yield. The yield could be increased to *ca* 80% and further to 95% reducing the total volume of water by a factor of 2 or 5 respectively. However, as expected, both the quality and size of crystals appeared to be strongly dependent upon concentration. For all three cases, the homogeneity of the polycrystalline sample, that is, presence of a pure phase was checked by PXRD measurements.

Synthesis of (2−2H$^+$)$_3$(M[(CN)$_6$]$^{3-}$)$_2$. 8H$_2$O) (M = Cr, Fe or Co). To an aqueous solution (distilled, 100 mL) of $K_3M(CN)_6$ (120 mg, 0.36 mmol) an aqueous solution (distilled, 100 mL) of **2**-2HCl·$2H_2O$ (180 mg, 0.470 mmol) was added. After two days, crystalline material was obtained. The latter was filtered and was dried in air affording the desired solid material in *ca* 55−60% yield. Again, the homogeneity of the polycrystalline samples was checked by PXRD measurements for all three cases.

2.2. Physical Measurements. Single-Crystal Studies. Data were collected at 173(2) K on a Bruker APEX8 CCD Diffractometer, equipped with an Oxford Cryosystem liquid N_2 device, using graphite-monochromated Mo−K_α (λ = 0.71073 Å) radiation. For all structures, diffraction data were corrected for absorption. The structures were solved using SHELXS-97 and refined by full matrix least-squares on F^2 using SHELXL-97. The hydrogen atoms were introduced at calculated positions and not refined (riding model).[24]

Powder Diffraction Studies (PXRD). PXRD diagrams were collected on a Scintag XDS 2000 diffractometer using monochromatic Cu Kα radiation with a scanning range (2 h) between 5 and 90° using a scan step size of 2°/mn.

Variable temperature powder diffraction studies were performed under static air on a Siemens D-5000 diffractometer (θ–θ mode, CoKα radiation, λ = 0.1789 Å) equipped with an Anton Parr HTK16 high temperature device and a M Braun linear position sensitive detector (PSD).

The dehydration−rehydration process has been studied in the 20−200−20 °C temperature range with 10 °C steps for (**2**-2H$^+$)$_3$([Co(CN)$_6$]$^{3-}$)$_2$·$8H_2O$ and in the 20−200−60 °C temperature range with 10 °C steps for (**2**-2H$^+$)$_3$([Co(CN)$_6$]$^{3-}$)$_2$·$8H_2O$. The delay between consecutive acquisitions was 40 min.

Thermogravimetric (TGA) Studies. TGA measurements have been performed on Pyris 6 TGA Laboratory System (Perkin-Elmer), using a N_2 flow of 20 mL/mn and a heat rate of 10 °C/mn.

DSC Studies. DSC measurements have been performed on a DSC Jade (Perkin-Elmer), using a N_2 flow of 20 mL/mn and a heat rate of 10 °C/mn except for the case of crystals containing cobalt for which both heat rate of 2 and 10 °C/ mn were imposed.

3. Results and Discussion

H-bonding, one of the most exploited ones,[6,7a,9] is a particular mode of interaction allowing to design a variety of recognition patterns. Its rather weak nature may be compensated by addition of more robust charge−charge electrostatic interactions.[16−22] We have, for some time now, explored this idea by combining H-bond donor cationic and H-bond acceptor anionic tectons.[17−22]

Scheme 1

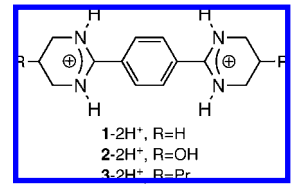

In particular, we have shown that dicationic tectons such as compounds **X**-2H$^+$, (**X** = **1**−**3**) (Scheme 1) are particularly well suited for the generation of charge-assisted H-bonded networks when combined with cyanometallate complex anions.[18−22] For example for compound **1**-2H$^+$, 1-D networks are obtained with dicyanometallates [M^{I}(CN)$_2$]$^-$ (M = Au or Ag),[18] tetracyanometallates [M^{II}(CN)$_4$]$^{2-}$ (M = Ni, Pd and Pt)[19] and pentacyanometallate [Fe^{II}(CN)$_5$NO].[20] The same tecton leads to the formation of 2-D networks when associated with hexacyanometallates [M^{III}(CN)$_6$]$^{3-}$ (M = Fe, Co, Cr) or [M^{II}(CN)$_6$]$^{4-}$ (M = Fe, Ru) anions.[19a,21]

By a systematic structural study using X-ray diffraction on single-crystals, we have shown that the combination of dicationic tectons such as **1**-2H$^+$[19a] and **3**-2H$^+$[21b] (Scheme 1) with [M^{III}(CN)$_6$]$^{3-}$ (M = Fe, Co, Cr) anions leads to the formation of honeycomb type neutral 2-D charge-assisted H-bonded networks presenting deformed hexagonal cavities (Figure 1). The observed connectivity and shape result from the 3/2 stoechiometry between the two complementary tectons which leads to a neutral system. The packing of the 2-D networks leads to the formation of porous crystals offering distorted hexagonal channels along the *a* axis.

In the case of **1**-2H$^+$, the channels, representing *ca* 16%[25] of the total volume of the crystal, are obviously not empty but filled with 7 water molecules (Figure 2a).[19a] These solvent molecules interact through H-bonds with anions (OH···N with O···N distance in the range of *ca* 2.85−2.95 Å) as donor or with other water molecules either as donor or acceptor (OH···O with O···N distance in the range of *ca* 2.80−2.85 Å). No interaction by H-bonding between the water molecules and the organic part of the network is observed. Among the 7 water molecules, one is disordered over two positions with an occupancy of 0.5, whereas the other six form 1-D networks though interconnection of hexagons by tetragons (Figure 4a).

In the case of **1**-2H$^+$, the three crystals obtained do not present the same crystallographic features (Figure 3). Indeed, whereas crystals based on [Co(CN)$_6$]$^{3-}$ and [Fe(CN)$_6$]$^{3-}$ are *iso*structural (*triclinic*, space group $P\bar{1}$, Figure 3a), for [Cr(CN)$_6$]$^{3-}$, the crystal shows a higher symmetry (*monoclinic*, space group $P2_1/n$, Figure 4b) (see Table 1 and Table S1 in the Supporting Information). This feature, corresponding to a flip of **1**-2H$^+$ units, is probably for steric reasons the consequence of the longer Cr−N distance (d_{Cr-N} = 3.24 Å, d_{Fe-N} = 3.09 Å, d_{Co-N} = 3.04 Å).

Based on the above-mentioned observations on **1**-2H$^+$, we have designed the tecton **3**-2H$^+$ bearing four propyl chains and demonstrated that, for steric reasons and by rendering the interior of the channels more hydrophobic, it is possible to prevent the inclusion of water molecules by occupying the channels by the propyl fragments (Figure 2c).[21b]

3.1. Design and Structural Studies. To demonstrate the possibility of increasing the hydrophilicity of the channels

(24) Sheldrick, G. M. *Programs for the Refinement of Crystal Structures*; University of Göttingen: Göttingen, Germany, 1996.

(25) Spek, A. L. *PLATON, A Multipurpose Crystallographic Tool*; Utrecht University: Utrecht, The Netherlands, 1998.

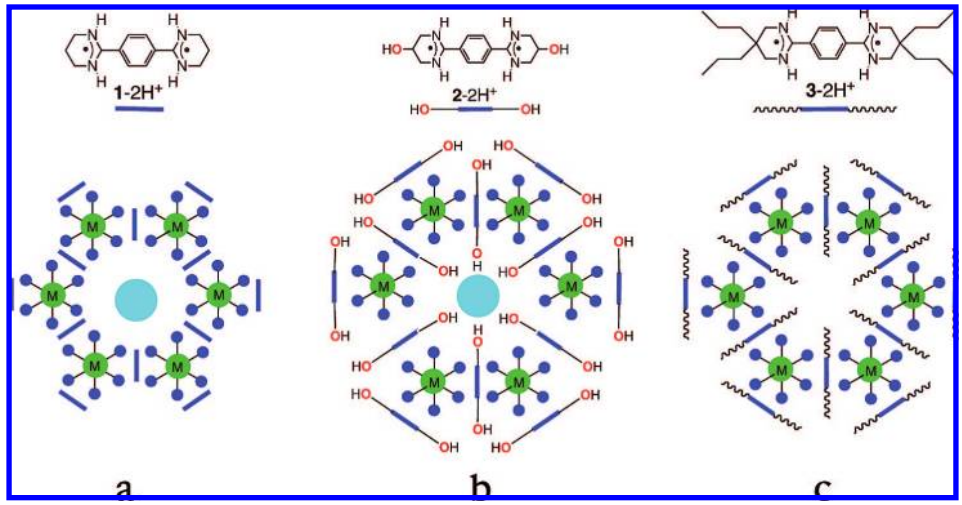

Figure 2. Schematic representation of 2-D honeycomb type charge-assisted H-bonded networks generated by combining tectons **X**-2H$^+$ (**X** = **1** (a); **X** = **2** (b); **X** = **3** (c)) with $[M(CN)_6]^{3-}$ (M = Fe, Co, Cr) anions. For **1**-2H$^+$and **2**-2H$^+$, the blue circle in the center of the cavity represents the water molecules.

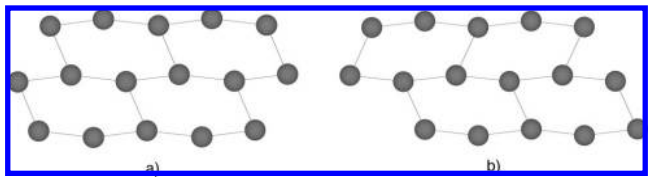

Figure 3. Schematic representations of the two types of 2-D networks obtained for the association of **1**-2H$^+$ with $[M(CN)_6]^{3-}$ anions: $P\bar{1}$ (a) for M = Fe and Co and $P2_1/n$ (b) for M = Cr. Grey circles represent the metal centers. The increase in symmetry in the case of Cr corresponds to a flip of **1**-2H$^+$ units. For **2**-2H$^+$, in all three cases *iso*structural crystals (b) are obtained.

(Figure 1), the tecton **2**-2H$^+$ was designed (Figure 2b). The latter, an analogue of **1**-2H$^+$, possesses two cyclic amidinium groups taking part in the recognition pattern as H-bond donor sites when combined with cyano groups of the cyanometallate. Furthermore, in order to bind water molecules in the channels and thus control their release and uptake, tecton **2**-2H$^+$ was decorated with two auxiliary OH groups at its both extremities pointing toward the interior of the pores. It is worth noting that owing to its less acidic character, the OH groups do not compete with amidinium sites and thus indeed behave as auxiliary groups.

Upon mixing an aqueous solution of potassium hexacyanometallate $K_3M(CN)_6$ (M = Fe, Co, Cr) and an aqueous solution of the diprotonated tecton **2**-2H$^+$ as its chloride salt, large quantities of crystalline materials were obtained for all three metal cations (see Table 2 and Table S2 in the Supporting Information). In each case, the homogeneity of the crystalline batch was confirmed by X-ray powder diffraction (PXRD) which revealed a single phase. For the sake of comparison, the same procedure was employed when using the tecton **1**-2H$^+$.

In all cases, the solid state structures of the crystalline materials were investigated by X-ray diffraction on single-crystals (Figure 4b). In contrast with the case of **1**-2H$^+$ for which crystals are composed of **1**-2H$^+$, $[M(CN)_6]^{3-}$ (M = Fe, Co, Cr) and 7 water molecules (Figure 4a), for **2**-2H$^+$, 8 water molecules are present in the lattice. The structural study revealed that crystals obtained with all three cations are *iso*structural (*monoclinic*, space group $P2_1/n$, Figure 3b). As expected from the design of **2**-2H$^+$, the cationic and anionic units are interconnected through both H-bonding and electrostatic interactions leading to the formation of neutral 2-D networks.

For the organic tecton **2**-2H$^+$, each cyclic amidinium moiety adopts the half-chair conformation. The phenyl ring connecting the two cyclic amidinium moieties is tilted with the NCCC dihedral angle in the range of −47 and 42°. The tecton is centrosymmetric and thus the two OH groups ($d_{C\text{-}OH}$ of *ca* 1.42 Å) pointing in opposite directions are localized above and below the main plane of the backbone. As expected from the difference in the pK_a values between the cyanometallate and the amidinium group, the acidic protons are localized on the latter (d_{C-N} of *ca* 1.32 Å, NCN angle of 121°). The dication/trianion stoichiometry is 3/2 and each hexacyanometallate is connected to three bisamidinium and conversely each **2**-2H$^+$ is connected to two $[M(CN)_6]^{3-}$. The recognition event between $[M(CN)_6]^{3-}$ anion and the cationic tecton **2**-2H$^+$ defining the nodes of the network occurs *via* a dihapto mode of H-bonding between two acidic protons localized on the same side of **2**-2H$^+$ and two adjacent cyanide groups of the metal complex ($d_{N\text{-}NC}$ of *ca* 2.85−2.90 Å).

This connectivity mode leads to the formation of neutral 2-D honeycomb type networks with a (6,3) topology[7a,26] with the OH groups pointing toward the interior of the cavity (Figure 2b). The 2-D networks are packed along the *a* axis in parallel mode and eclipsed fashion. Consequently, the crystal presents distorted hexagonal type channels which represent 12% of the total volume of the crystal.[25] This corresponds to 4% decrease when compared to **1**-2H$^+$ (16%).

The channels are filled with water molecules. Although the volume of the channels is decreased by 4% in the case of **2**-2H$^+$, the increase in the number of water molecules from 7 for **1**-2H$^+$ to 8 for **2**-2H$^+$ is due to the interactions through H-bonding between water molecules and OH groups. Indeed, whereas for **1**-2H$^+$, as stated above, the solvent molecules form only H-bonds between them and with CN groups of the cyanometallate units, in the case of **2**-2H$^+$, as expected by its design, three types of H-bonding take place, that is, HOH···NC (d_{O-N} in the range of 2.81−2.90 Å), HOH···OH (d_{O-O} in the range of 2.71−2.77 Å), H_2O···HOC (d_{O-O} in the range of 2.66−2.69

(26) (a) Wells, A. F. *Three-Dimensional Nets and Polyhedra*; Wiley-Interscience: New York, 1977. (b) Wells, A. F. *Further Studies of Three-dimensional Nets*, ACA Monograph No. 8; American Crystallographic Association: Buffalo, 1979. (c) Batten, S. T; Robson, R. *Angew. Chem., Int. Ed.* **1998**, *37*, 1460–1494.

Table 1. Short Crystallographic Parameters for (**1**-2H$^+$)$_3$([M(CN)$_6$]$^{3-}$)$_2$ 7 H_2O (M = Fe, Co, Cr) and Their Dehydrated Forms, Recorded at 173 K

	(1−2H$^+$)$_3$ ([Cr(CN)$_6$]$_2$)		(1−2H$^+$)$_3$([Fe(CN)$_6$]$_2$)		(1−2H$^+$)$_3$([Co(CN)$_6$]$_2$)	
formula	[H_2O]$_7$	dehydrated	[H_2O]$_7$	dehydrated	[H_2O]$_7$	dehydrated
Mwt	1275.37	1149.26	1283.07	1156.96	1289.23	1163.12
Crystal system	Monoclinic	Monoclinic	triclinic	triclinic	triclinic	triclinic
Space group	$P2_1/n$	$P2_1/c$	$P\bar{1}$	$P\bar{1}$	$P\bar{1}$	$P\bar{1}$
a (Å)	7.1142(4)	7.2563(3)	7.0949(3)	7.2138(6)	7.0982(4)	7.2141(4)
b (Å)	21.4319(13)	20.5934(9)	12.3765(5)	12.1706(11)	12.3509(7)	12.1497(8)
c (Å)	20.9403(13)	21.5442(9)	17.9534(7)	17.3090(16)	17.8586(10)	17.2052
α (deg)	90	90	83.580(2)	84.987(2)	83.535(2)	84.582(4)
β (deg)	91.702(2)	106.777(3)	87.6101(10)	89.044(3)	87.4280(10)	88.960(4)
γ (deg)	90	90	83.9340(10)	83.821(2)	83.967(2)	84.052(4)
V (Å^3)	3191.4(3)	3082.4(2)	1557.12(11)	1505.0(2)	1546.21(15)	1493.15(17)

Table 2. Short Crystallographic Parameters for (**2**-2H$^+$)$_3$([M(CN)$_6$]$^{3-}$)$_2$ 8 H_2O (M = Fe, Co, Cr) and Their Dehydrated Forms, Recorded at 173 K

	(2−2H$^+$)$_3$([Cr(CN)$_6$]$_2$)		(2−2H$^+$)$_3$([Fe(CN)$_6$]$_2$)		(2−2H$^+$)$_3$([Co(CN)$_6$]$_2$)	
formula	[H_2O]$_8$	dehydrated	[H_2O]$_8$	dehydrated	[H_2O]$_8$	dehydrated
Mwt	1389.39		1397.09	1252.96	1403.25	1259.12
Crystal system	Monoclinic	Monoclinic	Monoclinic	Monoclinic	Monoclinic	Monoclinic
Space group	$P2_1/n$	$P2_1/n$	$P2_1/n$	$P2_1/n$	$P2_1/n$	$P2_1/n$
a (Å)	7.1190(2)	7.2526(9)	7.0978(5)	7.2655(10)	7.1180(10)	7.2886(2)
b (Å)	22.3250(6)	19.894(3)	22.2254(16)	19.6845(18)	22.252(4)	19.5917(5)
c (Å)	21.0110(6)	20.773(3)	20.6357(12)	20.427(3)	20.508(4)	20.3127(5)
α (deg)	90	90	90	90	90	90
β (deg)	92.8190(17)	93.909(4)	92.363(3)	93.837(7)	92.239(6)	93.611(2)
γ (deg)	90	90	90	90	90	90
V (Å^3)	3335.27(16)	2990.2(7)	3252.5(4)	2914.9(7)	3245.8(10)	2894.81(13)

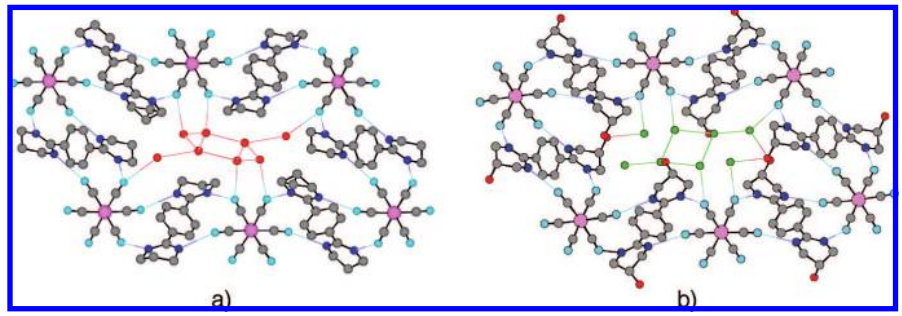

Figure 4. Portions, of the hydrated forms of *iso*structural crystals formed upon combining the tecton **1**-2H$^+$ with [M(CN)$_6$]$^{3-}$ (M = Fe, Co) (a) and **2**-2H$^+$ with [M(CN)$_6$]$^{3-}$ (M = Fe, Co, Cr) (b) showing the filling of channels along the *a* axis. For sake of clarity, H atoms are omitted. Dashed lines represent H-bonds. N atoms are differentiated by color (CN: pale blue, amidinium: dark blue). O atoms of H_2O molecules are colored in green in the case of **2**-2H$^+$.

Å) and finally $H_2O\cdots H_2O$ (d_{O-O} in the range of 2.70−3.02 Å). Concerning the organic part, among the six **2**-2H$^+$ units composing the cavity, four of them also interact with each other through H-bonds of the type OH···OH (d_{O-O} of *ca* 2.82 Å). In contrast with the case of **1**-2H$^+$, among the eight solvent molecules present in the cavity, six form discrete hexameric units (Figure 4b).

3.2. Dehydration/Rehydration. To have a reference case, the dehydration-hydration processes in the crystalline phase were studied by X-ray diffraction methods both in the case of **1**-2H$^+$ (Figure 5a, Table 1) and **2**-2H$^+$ (Figure 5b, Table 2). For both types of crystals, the dehydration was induced thermally upon heating the crystal to 180 °C (by 10 °C/mn steps) and the resulting dehydrated sample was studied by XRD on single-crystal. The homogeneity of the dehydrated phases was also confirmed by PXRD investigations on different batches. Several dehydration−rehydration cycles were performed and in all cases the initial number of water molecules (7 for **1**-2H$^+$ and 8 for **2**-2H$^+$) was observed by TGA analysis. In all cases, the dehydration−rehydration event takes place *via* single-crystal-to-single-crystal (SCSCT) transformation. Both for dehydrated crystals obtained with **1**-2H$^+$ or with **2**-2H$^+$, the 2-D neutral network structure is conserved. The connectivity between the cationic and anionic tectons is ensured by dihapto modes of H-bonding and electrostatic interactions. The organic tectons **1**-2H$^+$ (d_{N-NC} of *ca* 2.88−2.95 Å, Ph tilted with NCCC dihedral angle in the range of *ca* −47 and +42°) and **2**-2H$^+$ (d_{N-NC} of *ca* 2.80−3.02 Å, Ph tilted with NCCC dihedral angle in the range of *ca* −45 and +49°) exhibit the same type of conformation as for the hydrated forms. For **1**-2H$^+$ in the case of both Co and Fe, as for the hydrated form, the crystalline system (*triclinic*) and space group ($P\bar{1}$) remain identical whereas for dehydrated form obtained with Cr, the crystalline system (*monoclinic*) remains the same but the space group ($P2_1/c$) is different from the one observed for its hydrated form ($P2_1/n$) (Tab. 1). The comparison of the hydrated and dehydrated structures shows that a small decrease in the cell parameters takes place upon removal of water molecules (*ca* −4.1% volume

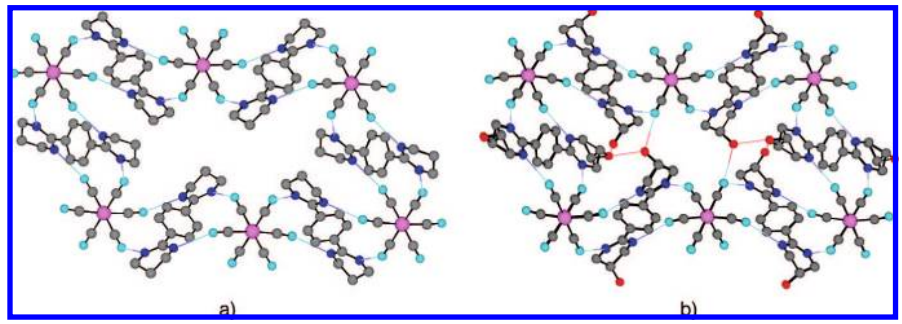

Figure 5. Portions along the *a* axis of the dehydrated forms of *iso*structural crystals formed upon combining the tecton **1**-2H$^+$ with $[M(CN)_6]^{3-}$ (M = Fe, Co) (a) and **2**-2H$^+$ with $[M(CN)_6]^{3-}$ (M = Fe, Co, Cr) (b). In the case of **2**-2H$^+$, 2 consecutive units are presented showing the formation of H-bonds between consecutive layers. Dashed lines represent H-bonds. For sake of clarity, H atoms are omitted. N atoms are differentiated by color (nitrile: pale blue, amidinium: dark blue).

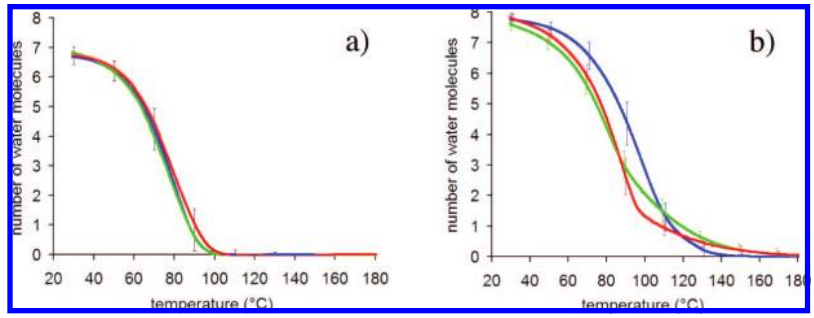

Figure 6. TGA curves obtained for $(\mathbf{1}\text{-}2H^+)_3[M(CN)_6^{3-}]_2$ (a) and $(\mathbf{2}\text{-}2H^+)_3[M(CN)_6^{3-}]_2$ (b) (M = Fe in red, Co in blue and Cr in green) showing the release of 7 and 8 H_2O molecules for **1**-2H$^+$ and **2**-2H$^+$, respectively.

shrinkage). The channels occupy *ca* 11% of the total volume of the crystal instead of *ca* 16% for the hydrated form.[25]

For **2**-2H$^+$ (Figure 5b) in all cases (Co, Fe, Cr), the same crystalline system (*monoclinic*) and space group ($P2_1/n$) are obtained for both dehydrated and hydrated forms (Table 2). However, in all three dehydrated forms (Co, Fe, Cr), for one of the three **2**-2H$^+$ units present in the asymmetric unit, the C atom bearing the OH group is disordered over two positions with an occupancy of 0.5. In marked contrast with **1**-2H$^+$, the dehydration process causes a significant compression along the *b* axis (−2.66 Å, that is, −12%). The cell volume is decreased by *ca* 10.8% and consequently almost no empty space is available in the channels, that is, 4% of the total volume of the crystal instead of 12%.[25] The shape of the cavity changes from deformed hexagonal to more rectangular. In contrast with the hydrated form for which H-bonds between OH groups are present within the cavity of the 2-D networks, for the dehydrated form, these interactions are absent. However, the dehydration process leads to the formation of H-bonds of the OH···OH and OH···NC types between consecutive 2-D networks. Indeed, for each rectangular shape unit, on each side, the OH groups pointing toward the next layer are interconnected ($d_{OH\text{-}OH}$ in the range of 2.79−2.88 Å). Furthermore, among the 6 OH groups, 2 are also H-bonded to the CN groups belonging to next layers ($d_{OH\text{-}NC}$ in the range of 2.81−2.85 Å). Thus, when taking into account all H-bonding patterns, the overall structure may be described as a 3-D network presenting rectangular type channels.

The cases reported here are rare examples of single-crystal-to-single-crystal-transformations in hydrogen bonded networks,[27] specially for hybrid organic/inorganic type networks.[16g]

(27) Fur, E. L.; Demers, E.; Marris, T.; Wuest, J. D *Chem. Commun.* **2003**, 2966–2967.

3.3. Thermal Behavior. As stated above, in comparison with **1**-2H$^+$, the tecton **2**-2H$^+$ possesses two additional OH moieties as H-bond donor/acceptor groups. As the result of the localization of these two moieties on the tecton's backbone, they are oriented toward the interior of the channels as confirmed by the structural study mentioned above (Figure 4). Thus, the generated channels must offer an increased hydrophilicity through the establishment of H-bonds with water molecules. Consequently, with respect to **1**-2H$^+$, water molecules must be more strongly retained in the channels formed in the presence of **2**-2H$^+$. This was indeed established by thermogravimetric analysis (TGA) on all six hydrated crystals (**X**-2H$^+$)$_3$([M(CN)$_6$]$^{3-}$)$_2$·yH_2O (**X** = **1** or **2**, M = Fe, Co, Cr, y = 7 or 8) (Figure 6). Although the thermal behavior for both dehydrated crystals obtained upon combining Fe and Cr based complex anions with tectons **1** or **2** was similar (decomposition at *ca* 240 °C), for the dehydrated material based on Co and **1** or **2**, crystals were found to be stable up to 300 °C. The TGA study on (**1**-2H$^+$)$_3$([M(CN)$_6$]$^{3-}$)$_2$·7H_2O (M = Fe, Co, Cr) in the 25−180 °C temperature range clearly indicates that, under the same conditions, independently of the nature of the central metal cation, the three solids behave in the same manner, that is, the 7 water molecules are evacuated at *ca* 100 °C (Figure 7a). Interestingly, under identical experimental conditions, in the case of (**2**-2H$^+$)$_3$([M(CN)$_6$]$^{3-}$)$_2$·8H_2O (M = Fe, Co, Cr), the complete dehydration process (loss of 8 water molecules) takes place at *ca* 140 °C (Figure 7b). This difference in temperature (ΔT) of *ca* 40 °C reflects in part stronger interactions between water molecules and the channels.

The dehydration event was also studied by Differential Scanning Calorimetry (DSC) for both types of solids (under N_2, 10 °C/minute). For the hydrated crystals composed of **1**-2H$^+$ and $[M(CN)_6]^{3-}{}_2$ (M = Fe, Co, Cr) and 7 H_2O, the DSC study

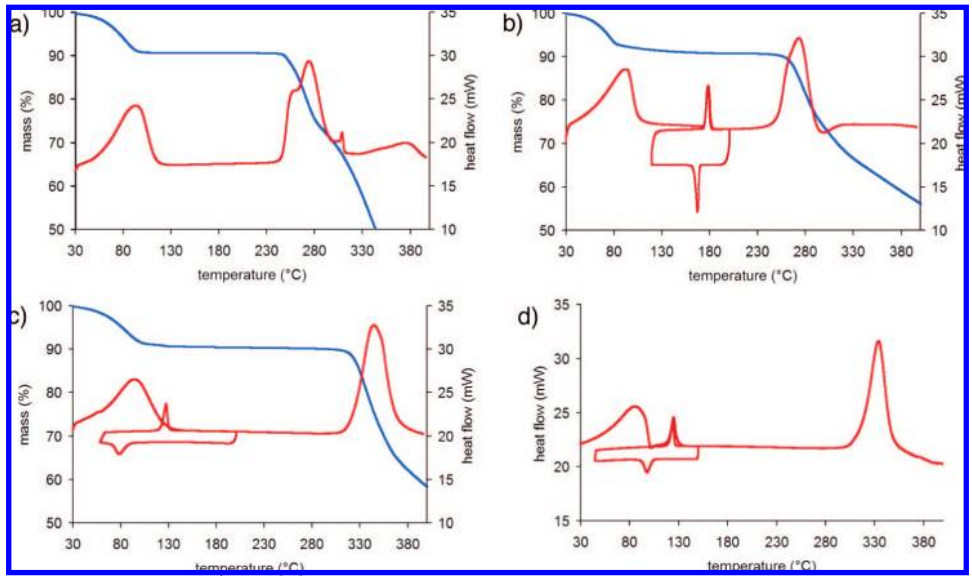

Figure 7. TGA (blue) and DSC (red) curves (10 °C/min) for (**1**-2H$^+$)$_3$[Co(CN)$_6^{3-}$]$_2$ 7 H_2O (a), (**2**-2H$^+$)$_3$[Fe(CN)$_6^{3-}$]$_2$ 8 H_2O (b), [**2**-2H$^+$]$_3$[Co(CN)$_6^{3-}$]$_2$ 8 H_2O (c) and for (**2**-2H$^+$)$_3$[Co(CN)$_6^{3-}$]$_2$ 8 H_2O with temperature steps of 2 °C/min (d), see text.

revealed an endothermic process at *ca* 95 °C corresponding to the loss of water molecules. The second endothermic process leading to the decomposition of the sample occurs at 240 °C for both Fe and Cr and at 300 °C for Co (see Figure 7a for Fe) respectively. Although unexpected, interestingly for (**2**-2H$^+$)$_3$([Fe(CN)$_6$]$^{3-}$)$_2$·8H_2O, DSC investigation indicated the presence of a phase transition occurring at *ca* 176 °C after the dehydration and prior to decomposition (Figure 7b). This process was found to be reversible. Indeed, starting at 25 °C, upon increasing the temperature, a first endothermic peak centered around *ca* 95 °C corresponding to the release of water molecules is observed. Further increase of the temperature to 200 °C (below the decomposition temperature) leads to the appearance of another endothermic process at *ca* 176 °C. Upon cooling to 120 °C (above the dehydration temperature), an exothermic process is observed at *ca* 170 °C. The surfaces under the two opposite peaks are roughly identical indicating the reversibility of the transition. Furthermore, upon reincreasing the temperature to 380 °C, the same endothermic peak was observed prior to decomposition. The same type of reversible process was also observed for (**2**-2H$^+$)$_3$([Co(CN)$_6$]$^{3-}$)$_2$·8H_2O although at different temperatures (Figure 7c). Indeed in that case, under the same conditions, upon heating the endothermic process occurs around 120 °C and the reverse transition takes place at *ca* 80 °C. Owing to the overlap between the peaks corresponding to the dehydration and the one resulting from the transition, the same process was studied at lower scan rate (2 °C/minute instead of 10 °C/minute). The latter study confirmed the similarity between Co and Fe (Figure 8d). However, under the same conditions, in the case of Cr, no such transition was observed.

3.4. Phase Transition in the Dehydrated Form. To study the dehydration/hydration process as well as the phase transition observed by DSC, variable temperature PXRD measurements were performed on both (**2**-2H$^+$)$_3$([Fe(CN)$_6$]$^{3-}$)$_2$·8H_2O, and (**2**-2H$^+$)$_3$([Co(CN)$_6$]$^{3-}$)$_2$·8H_2O crystals. Starting at 20 °C, the temperature was first increased to 200 °C and then decreased to 20 °C (10 °C steps, 40 min delay). For each temperature, the diffractogramm was recorded. The thermodiffractogramms for the Fe clearly indicate that the solid remains crystalline (Figure 9). Under these conditions, starting from the hydrated form, the increase of temperature to *ca* 50 °C induced the

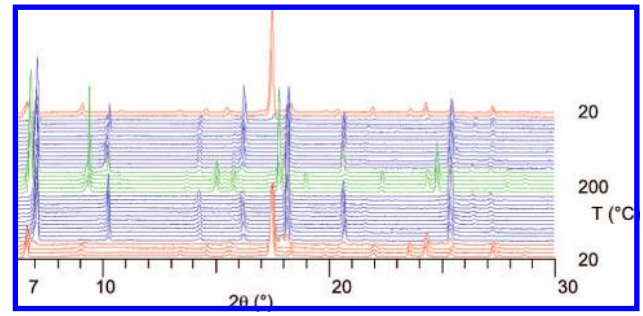

Figure 8. PXRD thermodiffractogramms obtained upon increasing/decreasing the temperature in the range of 20−200 °C for (**2**-2H$^+$)$_3$([Fe(CN)$_6$]$^{3-}$)$_2$·8H_2O. For clarity, different phases are differentiated by color (hydrated: red, first dehydrated: blue, second dehydrated: green).

dehydration process. This first dehydrated phase remained stable up to *ca* 170 °C. At that temperature, a new set of peaks corresponding to the second dehydrated phase was observed. The latter remained unchanged up to *ca* 200 °C. Upon cooling the sample, the reverse (appearance of the first dehydrated and then the hydrated phases) was observed confirming the reversibility of both hydration/dehydration processes and of the second phase transition.

The DSC measurements (appearance of the second phase transition at *ca* 180 °C) and the TGA trace (no loss of mass), suggest that the transition between the two dehydrated phases probably corresponds to the reorganization of the organic and inorganic tectons in the crystalline phase. Since no such a phenomenon was observed in the case of **1**-2H$^+$, implies that the OH groups pointing toward the interior of the channels are responsible for the reorganization. As stated above, based on X-ray structures of both hydrated and dehydrated forms, the removal of water molecules induces a change in the size and shape of the channels. Indeed, the initial distorted hexagonal shape channels are transformed into more rectangular ones upon dehydration. Based on the positions of peaks observed by the variable temperature PXRD study, the second dehydrated phase seems more similar to the hydrated form. This suggests that the reorganization of the H-bond patterns leads to more

hexagonal type channels. The same type of behavior was also observed for (**2**-2H$^+$)$_3$([Co(CN)$_6$]$^{3-}$)$_2$·8 H$_2$O crystals (see Figure S1 in the Supporting Information).

4. Conclusion

In conclusion, we have demonstrated that combinations of dicationic tectons **1**-2H$^+$ and **2**-2H$^+$ with [M(CN)$_6$]$^{3-}{}_2$ (M = Fe, Co, Cr) complex anions lead to the formation of robust neutral 2-D honeycomb type H-bonded networks presenting deformed hexagonal type cavities. The parallel packing of the 2-D networks in the eclipsed fashion generates stable porous crystals offering channels along the *a* axis. All six crystalline materials are hydrated and the water molecules are localized within the channels. All crystals are thermally robust and their decomposition temperature is in the range of 240−300 °C depending on the metal cation used. In all cases, the hydration/dehydration process, structurally studied on both forms by X-diffraction on single-crystals, is reversible and takes place through single-crystal-to-single-crystal transformations. The examples reported here represent rare cases of robust H-bonded networks undergoing reversible dehydration processes. As expected through the design of positively charged tectons **1**-2H$^+$ and **2**-2H$^+$, the introduction of two OH groups as additional H-bond donor/acceptor sites in **2**-2H$^+$ interferes with the release of water molecules with a ΔT of *ca* 40 °C between **1**-2H$^+$ lacking the OH moieties and **2**-2H$^+$. This proves the validity of the design principle. Indeed, it is possible to control the hydrophilic nature of the channels through the decoration of the tecton's backbone with appropriate auxiliary groups and thus the interactions between water molecules and the interior of the channels. Again, this aspect is rather unique and no such process has been reported previously in the literature. For **1**-2H$^+$, the thermal behavior for the dehydration process was similar and independent of the nature of the metal center. However, for **2**-2H$^+$, both in the case of Fe and Co, a reversible phase transition corresponding to a slight reorganization of interactions between positively charged tectons **2**-2H$^+$ and [M(CN)$_6$]$^{3-}{}_2$ complex anions (presumably through H-bonds engaging the OH groups) takes place after dehydration and prior to decomposition. In summary, this investigation clearly demonstrates two crucial features of crystal engineering: (i) through the design of molecular tectons the possibility of generating modular thermally robust porous H-bonded crystalline materials, (ii) the manipulation of properties of the solid material at the level of tectons leading to the control of the hydrophilicity of channels and consequently the release and uptake of water molecules. Work along the same lines, in particular with other types of organic tectons are currently ongoing. Furthermore, the proton conductivity of the reported solids will be investigated.

Acknowledgment. Dedicated to J.-M. Lehn on the occasion of his 70th birthday. Université Louis Pasteur, Institut Universitaire de France, the CNRS and the Ministry of Education and Research are acknowledged for financial support and for a scholarship to P.D. Dr. Thomas Devic and Guillaume Laugel are kindly acknowledged for their help with XRPD measurements.

Supporting Information Available: Figure S1: PXRD thermodiffractogram obtained upon increasing/decreasing the temperature in the range of 20−200−60 °C for (**2**-2H$^+$)$_3$([Co(CN)$_6$]$^{3-}$)$_2$·8 H$_2$O. For clarity, different phases are differentiated by color (hydrated: red, first dehydrated: blue, second dehydrated: green). Complete crystallographic tables for (**X**-2H$^+$)$_3$([M(CN)$_6$]$^{3-}$)$_2$·yH$_2$O (**X** = **1** or **2**, M = Fe, Co, Cr, *y* = 7 or 8) (Tables S1 and S2). This material is available free of charge via the Internet at http://pubs.acs.org.

JA806916T